Electrical Power and Energy Systems 158 (2024) 109937

Contents lists available at ScienceDirect

International Journal of Electrical Power and Energy Systems

journal homepage: www.elsevier.com/locate/ijepes

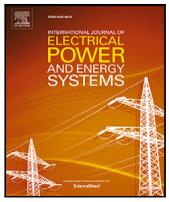

Multi-port coordination: Unlocking flexibility and hydrogen opportunities in green energy networks

Saman Nikkhah [a,*], Arman Alahyari [a], Abbas Rabiee [b], Adib Allahham [c], Damian Giaouris [a]

[a] School of Engineering, Newcastle University, Newcastle upon Tyne, NE1 7RU, UK
[b] Department of Electrical and Computer Engineering, Laval University, Quebec, G1V 0A6, Canada
[c] Faculty of Engineering and Environment, Northumbria University, Newcastle upon Tyne, NE1 8ST, UK

ARTICLE INFO

Keywords:
Multi-port coordination
Flexibility
Energy storage
Wind power penetration

ABSTRACT

Seaports are responsible for consuming a large amount of energy and producing a sizeable amount of environmental emissions. However, optimal coordination and cooperation present an opportunity to transform this challenge into an opportunity by enabling flexibility in their generation and load units. This paper introduces a coordination framework for exploiting flexibility across multiple ports. The proposed method fosters cooperation between ports in achieving lower environmental emissions while leveraging flexibility to increase their revenue. This platform allows ports to participate in providing flexibility for the energy grid through the introduction of a green port-to-grid concept while optimising their cooperation. Furthermore, the proximity to offshore wind farms is considered an opportunity for the ports to investigate their role in harnessing green hydrogen. The proposed method explores the hydrogen storage capability of ports as an opportunity for increasing the techno-economic benefits, particularly through coupling them with offshore wind farms. Compared to existing literature, the proposed method enjoys a comprehensive logistics-electric model for the ports, a novel coordination framework for multi-port flexibility, and the potentials of hydrogen storage for the ports. These unique features position this paper a valuable reference for research and industry by demonstrating realistic cooperation among ports in the energy network. The simulation results confirm the effectiveness of the proposed port flexibility coordination from both environmental and economic perspectives.

1. Introduction

Maritime transport plays a vital role in facilitating global trade. According to the UK's Department of Transport [1], a staggering 95% of UK imports and exports rely on seaborne transportation. Despite its pivotal role, this platform can contribute to several pressing global issues, such as environmental emissions with 2.89% of global greenhouse gas emissions in 2018 [2]. In 2019, the share of the UK domestic shipping sector alone in producing greenhouse gases was more than combined emissions from rail and bus transport [3]. These alarming issues could worsen in the future due to the operational and regulatory policies, potentially leading to even more dramatic consequences and higher levels of emissions. These challenges raised the global concerns over the operation of seaports.

Electrifying seaports is considered a pivotal solution to address this issue, and pave the way for a cleaner maritime industry. It can be a game-changing solution that can contribute to a more sustainable future [4], and integration of ports into the decarbonised energy network offers a multitude of benefits for ports and energy grid operators. Thanks to their strategic location, ports can serve as a host for different low or zero-emission technologies, such as renewable energy sources (RESs). Furthermore, due to the abundance of wind power generation available along the coastline, ports can play a vital role in increasing the utilisation of RESs. This strategic position also paves the way for the implementation of new technologies like green hydrogen, which can be a substantial fuel source for vessels. Given the logistical advantages of transmitting electric power over hydrogen, the seaports can produce hydrogen locally and employ it for fuel bunkering in the vessels.

Realising these opportunities can empower ports to achieve flexibility through an optimal asset and power management strategy, which considers both the logistics and electric operation of ports. Further potentials can be exploited thanks to digitalisation of ports, particularly via port networking, which can extend the potential for coordination of multiple ports [5]. The port networking is already a reality in some regions, where integrated platforms have been designed for port authorities, such as the integration platform proposed for mainland China [6]. The existence of such an integration platform underscores

* Corresponding author.
E-mail address: saman.nikkhah@newcastle.ac.uk (S. Nikkhah).

https://doi.org/10.1016/j.ijepes.2024.109937
Received 13 November 2023; Received in revised form 27 January 2024; Accepted 8 March 2024
Available online 15 March 2024

Nomenclature

Indices

b, i, j	Index of the main grid or the port network buses.
c	Index of cranes.
e	Index of IEVs.
r	Index of reefers.
t	Index of time.
v	Index of vessels.

Sets

Ω_b^s	Set of port network buses connected to the main grid.
Ω_c	Set of cranes.
Ω_e	Set of IEVs.
Ω_g	Set of buses connected to the thermal generation units.
Ω_p	Set of buses connected to port networks.
Ω_r	Set of reefers.
Ω_v	Set of vessels at berth.
Ω_{p2h}	Set of port network buses connected equipped with electrolyser.
Ω_t	Set of time periods.
Ω_{wt}	Set of WT connected buses.

Parameters

$S_{bj}^{Line_{\max/\min}}$	Maximum/minimum limit of power flow of the main grid transmission lines.
$V_b^{\max}$	Maximum value of the voltage magnitude.
$(P/Q)_b^{G_{\max/\min}}$	Maximum/minimum active/reactive power output of thermal generation units.
$(P/Q)_{b,t}^{P_{base}}$	Base active/reactive power consumption of the ports.
$(p/q)_{i,t}^{D}$	Miscellaneous active/reactive load inside the port.
$(p/q)_{i,t}^{G}$	Available active/reactive power generation inside the port.
$(r/x)_{ij}$	Resistance/reactance of branch ij of the port network.
Δt	Duration of time periods.
$\eta_{(c/d)}^{H}$	Charge/discharge efficiency of hydrogen tank connected to the electrolyser.
$\eta_{ch/dch}^{BES}$	Charge/discharge efficiency of BES.
$\eta_{ch/dch}^{IEV}$	Charge/discharge efficiency of IEV battery.
$\gamma_{0,i}, \gamma_{1,i}$	Cost coefficient of P2H units.
$\kappa_{0,i}, \kappa_{1,i}$	Hydrogen price.
$\lambda_b^{Op/Cr}$	Operational and curtailment price of wind power.
$\lambda_{b,t}^{p}$	Hourly price of providing flexibility by the ports.
λ_t^{O}	Ports supply curve price vector
ρ_e^{IEV}	Load factor of IEV e.
$\sigma_t^{e/v}$	Electricity/carbon emission price at time t.
$\varepsilon_b^{-/+}$	The coefficients for upper and lower values of reactive wind power.
$\vartheta_{b,\max}^{Flex}$	Maximum flexibility provided by each port.
ξ_i^{P2H}	Efficiency of electrolyser.
$\xi_{i,\max/\min}^{P2H}$	Maximum/minimum efficiency of electrolyser.
$a_{2,b}, a_{1,b}, a_{0,b}$	Coefficients of thermal generation units' cost function.
D_t	Flexibility demand
$E_e^{IEV_{\max}}$	Maximum energy capacity of IEV.
$i_{ij,\max}$	Maximum current flow of the port network.
N_c^{IEV}	Number of IEVs allocated to crane c.
N_v^{staff}	Number of staff assigned to each vessel.
O_t^{p}	Vector of port offers
$p_e^{IEV_{ch/dch}^{\max}}$	maximum charging/discharging power of IEV.
$P_{b,t}^{D}$	The main grid demand.
$P_{b,t}^{WT_a}$	Available wind power.
$p_c^{\max}$	Maximum power consumption of the crane.
$p_{i,max}^{BES-h/dch}$	Maximum charge/discharge power of BES.
$p_{r,max}^{\text{Reef}}$	Maximum power consumption of reefer r.
$p_{v,tot}^{Ves}$	Total load of vessel v.
$p_{v,t}^{Ves}$	Vessel load at time t.
$R_b^{(U/D)_G}$	Ramp up/down of thermal generation units.
$SOC_{i,max}^{BES}$	Maximum state of charge of BES.
$T_{r,\max/\min}^{Reef}$	Maximum/minimum internal temperature of reefer.
$T_{r,t}^{\text{amb}}$	Ambient temperature.
wf	Workforce cost at the port.
λ_G^{Em}	Emission price.
λ_G^{Res}	Price of spinning reserve provided by the thermal generation units.
ϕ_{Res}	Percentage of spinning reserve requirement based on the total system load.
$\varepsilon_b^{G_{Em}}$	Coefficient of thermal generators emission production per MW.

Variables

$S_{bj,t}^{Line}$	Power flow between the main grid buses b and j.
$(p/q)_{i,t}^{MG}$	Active/reactive power imported from the main grid to the port.
$(p/q)_{i,t}^{P2H}$	Active/reactive power consumed by electrolyser for producing hydrogen.
$(p/q)_{i,t}^{Reef}$	Reefer active/reactive power consumption.
$(p/q)_{ij,t}$	Active/reactive power flow of the branch ij of the port network.
$(V/\theta)_{b,t}$	Voltage magnitude of bus b in the main grid.
$(v/u)_{i,t}$	Voltage magnitude/squared voltage at node i of the port network.
$(Y/\phi)_{bj}$	Magnitude/angle of bj element of the main grid admittance matrix.
$\chi_{i,t}^{BES_{ch/dch}}$	Binary variable indicating charge/discharge power of BES.
$\chi_{c,v,t}^{Cr}$	Binary variable indicating the allocation of cranes to vessels.
π_t	Flexibility clearing price

the need for a coordination architecture that fosters cooperation between ports. Such cooperation can yield numerous advantages such as better use of assets, competition, and environmental benefits [7]. Thanks to these advancements, the coordination can enable higher levels of flexibility for the electrified ports as an integral part of the broader energy network.

$\vartheta_{b,t}^{Flex}$	Variable representing the percentage of port flexibility.
$E_{e,t}^{IEV}$	Energy stored at IEV battery.
G_t^p	Vector of accepted offers from all ports
$H_{i,t}$	Hydrogen extracted by electrolyser.
$i_{ij,t}$	Current magnitude of the branch ij of the port network.
$P_{b,t}^G$	Power output of thermal generation units.
$P_{b,t}^{P_{Res}}$	The power provided by the port for spinning reserve.
$P_{b,t}^{WTi/c}$	Injected/curtailed wind power.
$p_{c,v,t}^{Cr}$	Power consumption of crane c for unloading vessel V at time period t.
$p_{e,t}^{IEV_{ch/dch}}$	Charge/discharge power of IEV.
$p_{i,t}^{BES_{ch/dch}}$	Charge/discharge power of BES.
$p_{i,t}^{CHE}$	CHE power consumption.
$p_{i,t}^{BES_{ch/dch}}$	Charge/discharge power of the BES installed in the port.
$p_{r,t}^{\text{Reef}}$	The power consumption of reefer r.
$SOC_{i,t}^{BES}$	State of charge of BES.
$T_{r,t}^{Reef}$	Internal temperature of reefer.
y_t	Auxiliary variable for the demand unfulfilled by ports
$P_{b,t}^{G_{\text{Res}}}$	Spinning reserve provided by thermal generation units.
$P_{b,t}^{P_{\text{Res}}}$	Spinning reserve provided by port flexibility.

Consideration of various logistics and electrical constraints, the challenge of optimising the port operation has been addressed through the development of different optimisation problems in the literature. This challenge has been addressed through the development of various port asset management strategies. Research conducted in [8–10] shows the importance of effective power and asset management strategies in the context of smart ports. A mixed integer linear programming (MILP) model is introduced in [11] for optimal energy management of port assets including energy storage. The introduction of hybrid battery energy storage (BES) in [8] for shipboard microgrids has offered multiple advantages in terms of speed management, generation cost, and power management compared to battery-only systems. Notably, authors in [9] suggested an energy management strategy for optimal controlling of power generation and ship speed in a voyage without the need for additional investment in BES. Also, in [10], vessel arrival and speed management strategies are introduced to minimising the operational costs while accounting for the variation in arrival time.

It is shown in [12] that an optimised port operation can reduce reliance on the main grid power supply by 27.47% while decreasing the emission caused by vessels by 51.44%. A multi-objective cooperative framework is introduced in [13] for optimal operation management of shipping and port companies, which resulted in 3.8% emission and 35.9% cost reduction. Hein et al. [14] introduced an operation scheduling problem for optimal energy management of port assets considering multiple economic and environmental constraints. An energy hub management strategy is introduced in [15] for port assets using the economic dispatch method, with results demonstrating the cost and emission reduction. The authors in [16] investigated the importance of adding smart characteristics to the ports through the evaluation of a smart port index, considering the seaport as a microgrid.

Optimising port operations should yield benefits not only for the ports themselves but also for the broader energy grid, to which ports are primarily connected via the electric network. A recent research work published by Chen et al. [17] studies the issues around voltage fluctuation in port energy networks, where a multi-objective volt/VAR methodology is proposed to reduce voltage violation while pursuing economic goals. Authors in [18] proposed a real-time distributed demand response for hierarchical control of electrified ports. The authors focused on controlling the refrigerated containers and ship power supply as the flexibility options, using fuzzy decision making which is proved to be computationally demanding and requiring multiple alpha-cuts [19]. An integration framework is introduced in [20] for studying the flexibility options that could be provided with the multi-energy ports equipped with RESs and storage units. An optimal power management strategy is introduced in [21] for maximising the flexibility of port operation with consideration for reefers, electric vehicles, and cold ironing as the flexibility sources. Authors used particle swarm optimisation for solving local optimisations, which is proved to be computationally complex in terms of falling into local optimum solutions and a having low convergence rate [22]. A flexible voyage scheduling problem is proposed in [23] for improving the resilience of microgrids. Ref. [24] proposed a distributed voltage control method for decreasing the voltage violation effects caused by the all-electric ships considering the power interaction between the seaport microgrid and ships. A distribution system is adopted in [23,24] as the test seaport which may not be a representative of their logistics-electric operation. The potential of shipping containers to provide reactive power requirements of the on-shore power system is investigated in [25]. Authors in [26] investigated the role of battery BES in increasing the flexibility of the seaports.

Although optimising the operation of seaports and their flexibility have been studied in the literature,several important aspects need further investigation. Based on the literature review, the primary gaps identified in the existing research are:

- While logistics optimisation models have been created, there is a lack of development in understanding the interconnected operation of various assets (e.g., cranes and reefers) and integration of such logistics optimisation into the electricity system model. Hence, there is a need for a holistic logistics-electric model for port operations to explore the interdependence between the port and its corresponding electricity network.
- Although previous research works have explored port flexibility, the predominant focus has been on optimising power management at the individual port level. A comprehensive port flexibility framework should extend its scope to encompass the optimal management of assets within a logistics-electric model, while incorporating a coordination framework that facilitates the collaboration of multiple ports.
- Existing literature primarily examines the power exchange between a port and the broader electricity network, overlooking the significance of the main grid's physical and operational constraints. A paradigm shift is necessary to comprehensively explore port flexibility within a broader energy network. This shift involves incorporating the physical constraints of the electricity network and considering ports as integral components within a comprehensive system approach.
- The proximity of ports to offshore wind farms opens opportunities for leveraging green hydrogen, creating a mutually beneficial scenario by enhancing the penetration of wind power generation in the energy network. Although this is well-debated as a future direction of research, such a geographical potential requires further investigation.

Moreover, it is imperative to investigate the port flexibility within the broader context, acknowledging the port network integration into the whole energy system. A paradigm shift is required to encompass the physical constraints of the electricity network while considering ports

as an element of such a comprehensive system approach. Finally, ports' proximity to offshore wind farms can present opportunities for harnessing green hydrogen, while offering mutually beneficial outcomes by simultaneously increasing the penetration level of wind power generation in the energy network.

In this study, a multi-port coordination framework is proposed for exploiting flexibility in a whole energy system approach. This framework takes into account the intricate logistics and electric constraints within each port while accounting for the main operational and physical limits of the wider energy grid. The proposed method introduces the green port-to-grid (GP2G) concept, which enables seaports to optimally manage their asset operation as well as their cooperation with the regional ports so as to provide flexibility for the main grid. The mathematical model integrates the electric constraints of port operation with logistic asset port operation considering different assets inside the port such as reefers, cranes, vessels, BES, etc. In the proposed coordination framework, the required flexibility and possible wind power curtailment are obtained through an optimisation model which is solved by the main grid operator (MGO), and the obtained results are communicated to the port coordinator. Simultaneously, port operators send their supply curves to the port coordinator, where an optimisation problem is solved to define the value and price of flexibility for each port. This novel coordination scheme introduces green hydrogen production as a potential option for ports, capitalising on their strategic location near offshore wind farms to maximise the utilisation of RESs. With a logistics-electric model, this multi-port coordination paradigm provides a tangible demonstration of how port coordination can generate higher levels of flexibility, reduce environmental emissions, and realise economic benefits. Moreover, this paradigm can serve as a blueprint for ongoing and future projects. It fosters coordination of ports and their potential flexibility within a holistic energy system approach, allowing collaboration of different stakeholders in achieving a range of objectives. Generally, the main contributions of this paper are:

- A GP2G concept is introduced which incorporates the comprehensive logistics-electric model of ports, facilitating seamless integration of port flexibility into the energy grid. Such a model provides a realistic demonstration of how ports operate within the broader energy network, and it can be practically beneficial in studying future smart ports. Exploiting the flexibility of ports requires a well-defined integration architecture that considers the dynamic interaction of a wider energy grid.
- A multi-port coordination framework is introduced aiming at investigating the cooperation of ports in achieving environmental and economic objectives while integrating their flexibility into the main grid. This paradigm facilitates the cooperation of geographically dispersed ports, which can enable competition, and improve the operational efficiency of port operation through promoting their connectivity.
- A power to hydrogen (P2H) optimisation model is proposed based on availability of vessels at berth to increase wind power penetration. Expanding the port infrastructure along the coastlines enables the ports to prevent the curtailment of renewable power generation while delivering environmental and economic benefits for port authorities. The proposed coordination method outlines the production and storage of hydrogen for decreasing wind power curtailment. It enables investigation of how vessel arrival times, as a logistics parameter, affect hydrogen production within electrified port networks.

The remainder of this paper is organised as follows: Section 2 explains the framework of the proposed multi-port market-based coordination. Mathematical formulation is introduced in Section 3. Section 4 explains the process of solving the coordination optimisation framework. Section 5 provides the simulation setup and case studies. The simulation results are discussed in Section 6. Finally, Section 7 concludes the paper.

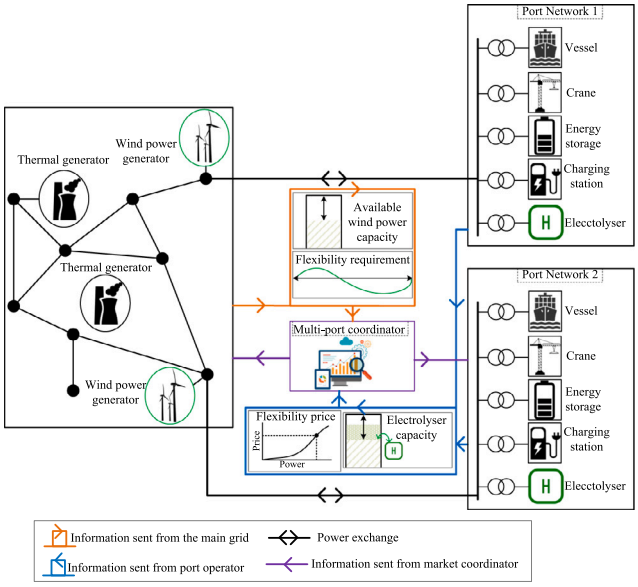

Fig. 1. Conceptual illustration of the proposed multi-port coordination scheme.

2. Multi-port coordination for decarbonisation

Digitisation of seaports represents a significant step towards their decarbonisation. By electrifying the port assets and introducing different distributed energy resources (DERs), the potential for enabling flexibility within the operation framework of seaports can be realised. This flexibility can be seamlessly integrated into the broader energy grid, where system planners can delay generation and transmission planning through optimal utilisation of flexibility resources [27]. Efficient utilisation of port flexibility, however, necessitates the development of a comprehensive framework that takes into account the objectives and constraints of both the main grid and the port.

Realising port flexibility entails the implementation of intelligent networks and operation control strategies. As ports become an integral component of future interconnected smart grids, port operation is intricately reciprocal to grid operation and vice versa. Electrification of ports' energy demand changes the dynamics between ports, shifting from a purely logistics-based mode to a logistics-electric connection. These advances, however, add complexity to the management of port operations, transforming it into a multi-vector problem. This transformation requires intelligent asset management and coordination between ports themselves, and their interaction with the energy network.

This study proposes a multi-port coordination framework designed to enable cooperation between geographically dispersed ports, aiming at emission and cost reduction for ports while providing flexibility for the broader energy network through the concept of GP2G. Fig. 1 depicts the conceptual definition of the proposed multi-port coordination scheme. The key element in this architecture is the coordinator, which oversees and optimises cooperation between the ports. Initially, the MGO runs its optimisation problem to minimise its overall cost encompassing the operational, emission, and wind power curtailment expenses. At the same time, the port operators run their own optimisation models to maximise their flexibility.

Following this, the MGO communicates the cumulative flexibility required from the ports, the surplus wind power generation (which could be potentially used for generating green hydrogen), and the maximum

acceptable price for the flexibility to the port coordinator. The port coordinator also receives individual supply curves from each port. The supply curves are generated based on available resources and asset management within the individual ports. Leveraging this information, the multi-port flexibility coordinator (MPFC) employs a cooperative algorithm to define the price and quantity of flexibility that should be contributed by each port. The primary objective of this platform is achieving lower levels of emission in achieving environmental policies.

The excess wind power generation reported by the MGO is also communicated to the ports for hydrogen production and storage. This multifaceted paradigm enables the numerous environmental, operational, and economic potentials within the broader energy grid [28]. This unique characteristic empowers ports to be active participants in the energy network through the provision of flexibility. The MPFC defines the required flexibility from each port, with consideration for the logistics setting of each port such as the arrival time of vessels, and available shiftable reefer demand. Additionally, it defines the price of flexibility based on the price cap established by the MGO while defining the available capacity for using wind power generation through P2H. Such a coordination method has multiple practical advantages:

- Decreasing the MGO expenses on the wind curtailment and minimising wind turbine shutdowns. [29].
- Enabling the cooperation of regional ports to collectively pursue various goals.
- Decreasing the need for generation and transmission investment in the main grid.
- Highlighting the pivotal role of ports in producing hydrogen, which can serve as a fuel for advancing green maritime initiatives.
- Enabling seaports to actively engage the flexibility market.
- Realising the environmental requirements for the future electrified smart ports.

3. Problem formulation

The proposed port flexibility coordination problem is a multi-stage optimisation. It begins with the MGO optimisation, where they solve their optimisation and communicate the flexibility requirements to the MPFC. Simultaneously, the port operators run an internal optimisation and send the supply curves to the MPFC. The MPFC carries out a third optimisation based on the data received from ports and MGO to define the flexibility price for each hour of operation. This section provides a mathematical description of the optimisation models solved by each operator. Detailed symbols and their meanings are provided in the Nomenclature section for reference. It should be noted that the parameters and variables representing the power consumption/generation of the main grid are represented with capital letters while those of ports are represented with lowercase letters.

3.1. The main grid optimisation

In the proposed coordination problem, the MGO aims at minimising the operational, emission, and wind curtailment costs, as well as the spinning reserve costs, while satisfying system physical constraints. The main grid load is supplied by the thermal generators and wind turbines, and MGO can utilise the flexibility provided by the ports in conjunction with the thermal generators to satisfy the required spinning reserve without resorting to load curtailment in the event of potential contingencies. The objective function of the MGO is defined below:

$$\begin{aligned}\min_{DV} OF^{MGO} &= \min\left\{\left(C^{Op}_{ThG}+C^{Op}_{WT}+C^{Cur}_{WT}+C^{\mathrm{Res}}_{GP}\right)+C^{Em}_{ThG}\right\}\\ &= \Delta t\left(\sum_{t\in\Omega_t}\sum_{b\in\Omega_G} a_{2,b}\left(P^G_{b,t}\right)^2+a_{1,b}P^G_{b,t}+a_{0,b}\right)\\ &\quad+\Delta t\left(\sum_{t\in\Omega_t}\sum_{b\in\Omega_{WT}}\lambda^{Op}_b P^{WT_i}_{b,t}\right)\\ &\quad+\Delta t\left(\sum_{t\in\Omega_t}\sum_{b\in\Omega_{WT}}\lambda^{Cr}_b P^{WT_c}_{b,t}\right)\\ &\quad+\Delta t\left(\sum_{t\in\Omega_t}\left(\sum_{b\in\Omega_G}\lambda^{\mathrm{Res}}_G P^G_{b,t}+\sum_{b\in\Omega_P}\lambda^{P_{\mathrm{Res}}}_t P^{P_{\mathrm{Res}}}_{b,t}\right)\right)\\ &\quad+\Delta t\left(\sum_{t\in\Omega_t}\sum_{b\in\Omega_G}\lambda^{Em}_G\varepsilon^{G_{Em}}_b P^G_{b,t}\right)\end{aligned} \tag{1}$$

where the first term in (1) corresponds to the operational cost associated with the thermal generation units. The second and third terms are indicatives of the operational cost and curtailment cost of WT respectively. The fourth term reflects the costs related to ensuring spinning reserve availability. The last term is the emission cost stemming from the operation of thermal generation units. At the main grid level, this objective function is optimised subject to the power flow and adhering to physical network constraints.

3.1.1. The main grid constraints

Investigating the potential flexibility of the ports requires a detailed demonstration model of the main grid, which, notably, has been missing in the existing literature [18]. The port flexibility can present notable potentials for its utilisation within the upper grid to which they are linked. In this paper, port flexibility is considered a sustainable alternative to supplant thermal generators in providing the spinning reserve. Considering the participation of ports in providing a specific level of spinning reserve, the subsequent constraints are considered for the main grid ($\forall b \in \Omega_b$).

$$\begin{aligned}&P^G_{b,t}+P^{WT}_{b,t}-P^D_{b,t}-P^{P_{base}}_{b,t}\\ &=V_{b,t}\sum_{j\in\Omega_b}V_{j,t}Y_{bj}\cos(\theta_{b,t}-\theta_{j,t}-\phi_{bj})\end{aligned} \tag{2}$$

$$\begin{aligned}&Q^G_{b,t}+Q^{WT}_{b,t}-Q^D_{b,t}-Q^{P_{base}}_{b,t}\\ &=V_{b,t}\sum_{j\in\Omega_b}V_{j,t}Y_{bj}\sin(\theta_{b,t}-\theta_{j,t}-\phi_{bj})\end{aligned} \tag{3}$$

$$P^{G_{\min}}_b \le P^G_{b,t} \le P^{G_{\max}}_b \tag{4}$$

$$Q^{G_{\min}}_b \le Q^G_{b,t} \le Q^{G_{\max}}_b \tag{5}$$

$$V^{\min}_b \le V_{b,t} \le V^{\max}_b \tag{6}$$

$$S^{Line_{\min}}_{bj} \le S^{Line}_{bj,t} \le S^{Line_{\max}}_{bj} \tag{7}$$

$$-R^{D_G}_b\times\Delta t \le (P^G_{b,t}-P^G_{b,t-1}) \le +R^{U_G}_b\times\Delta t \tag{8}$$

where constraints (2) and (3) are active and reactive power balance equations respectively, encompassing the contribution of WTs in load supply and the power consumption of ports. Constraints (4) and (5) represent the limits on the thermal generation units' output. Constraint (6) shows the upper and lower limits of the bus voltage magnitude. The apparent power flowing through the branches is limited by (7). Finally, the ramp-rate limits of thermal generation units is given in (8). To achieve computational efficiency, the main grid non-linear equations are linearised in accordance with [30].

3.1.2. Spinning reserve constraints

The availability of a spinning reserve is one of the critical challenges power system operators deal with. Maintaining a designated spinning reserve level during the system operation to prevent major outages in the system after an excursion or contingencies. This study delves into utilisation of the flexibility provided by the ports as a clean source of spinning reserve, thereby diminishing the need for using thermal generation in providing this service. Therefore, the spinning reserve constraints are represented as below:

$$0 \le \phi_{\mathrm{Res}} \times \sum_{b\in\Omega_b} P^{D}_{b,t} \le \left(\sum_{b\in\Omega_G} P^{G_{\mathrm{Res}}}_{b,t} + \sum_{b\in\Omega_P} P^{P_{\mathrm{Res}}}_{b,t} \right) \tag{9}$$

$$0 \le P^{G_{\mathrm{Res}}}_{b,t} \le \left(P^{G_{\max}}_{b} - P^{G}_{b,t} \right) \tag{10}$$

$$0 \le P^{P_{\mathrm{Res}}}_{b,t} \le \vartheta^{Flex}_{b,t} \times P^{P_{base}}_{b,t} \tag{11}$$

$$0 \le \vartheta^{Flex}_{b,t} \le \vartheta^{Flex}_{b,\max} \tag{12}$$

Constraint (9) shows the spinning reserve requirement delivered jointly by the ports and the thermal generation units based on the percentage of total system load (i.e. ϕ_{Res}). Constraint (10) limits the capacity of reserve offered by the thermal generation units, maintaining it within bounds of maximum power and scheduled amount. Constraint (11) denotes the spinning reserve provided by the port flexibility, determined by variable $\vartheta^{Flex}_{b,t}$, which is limited by constraint (12). Constraints (11) and (12) define the amount of spinning reserve that could be provided by the ports.

3.1.3. Wind turbine constraints

Wind power generation plays a vital role in achieving a sustainable economy. The variability of this energy source, however, is deemed an important challenge for system operators, where they have to curtail wind power to preserve system stability. This study tries to minimise wind power curtailment (as represented in Eq. (1)) through utilisation of port flexibility and the possibility of extra wind power to supply the electrolyser for producing hydrogen. From the main grid point of view, it is necessary to consider the injected wind power to the grid along with the curtailed power of these units, as represented in the following.

$$P^{WT_i}_{b,t} + P^{WT_c}_{b,t} = P^{WT_a}_{b,t} \tag{13}$$

$$0 \le P^{WT_i}_{b,t} \le P^{WT_a}_{b,t} \tag{14}$$

$$0 \le P^{WT_c}_{b,t} \le P^{WT_a}_{b,t} \tag{15}$$

$$\varepsilon^{-}_{b} \times P^{WT_i}_{b,t} \le Q^{WT}_{b,t} \le \varepsilon^{+}_{b} \times P^{WT_i}_{b,t} \tag{16}$$

where Eq. (13) denotes that the sum of injected and curtailed wind power to the grid is equal to the available wind power generation. The injected and available wind power is limited by constraints (14) and (15). Constraint (16) shows the reactive power limit of the wind turbine.

3.2. The port network optimisation

Coordination of port assets in a logistics-electric model to achieve environmental and economic benefits while providing flexibility for the wide energy grid requires the port operators to solve an optimisation problem. In this study, the port agents solve their own optimisation models and define a supply curve that shows the value of their flexibility. The objective function of the port optimisation networks comprises of cost of importing power from the main grid, emission cost, workforce cost, and the operational cost of producing hydrogen, minus the revenue from supplying hydrogen. The port network objective function is defined as below:

$$\min_{DV} OF^{port} = \sum_{t\in\Omega_t} \Delta t \times \left(C^{port}_{t} - R^{port}_{t} \right) \tag{17}$$

$$\begin{aligned} C^{port}_{t} &= \sum_{v\in\Omega_v} \sum_{c\in\Omega_c} \left(wf \times N^{staff}_{v} \times \chi^{Cr}_{c,v,t} \right) \\ &+ \sum_{ij\in\Omega^{s}_{b}} \left((\sigma^{e}_{t} + \sigma^{v}_{t}) \times p_{ij,t} \right) + \sum_{i\in\Omega_{p2h}} \left(\gamma^{p2h}_{0,i} + \gamma^{p2h}_{1,i} p^{P2H}_{i,t} \right) \end{aligned} \tag{18}$$

$$R^{port}_{t} = \sum_{i\in\Omega_{p2h}} \left(\kappa^{p2h}_{0,i} + \kappa^{p2h}_{1,i} H_{i,t} \right) \tag{19}$$

where in (18) the first term represents the workforce cost which is defined based on staff required per operating crane, the second term is the environmental and operational cost of importing power from the main grid, and the third term shows the operational cost of producing hydrogen. Eq. (19) represents the revenue from selling the hydrogen.

3.2.1. Port network constraints

Despite available literature [21], this study considers an electrical network for modelling the operation of the seaports. The realistic PoT is considered as the test system. Based on the future scenarios considered for decolonisation [31], this port is equipped with battery energy storage (BES), cargo handling equipment (CHE) comprising of both mains-connected cranes and hoppers, and battery-powered industrial electric vehicles (IEVs) (e.g. container tractors and reach stackers), reefers, and electrolysers. Considering these technologies, the DistFlow branch equations given in [32] are utilised to model the power flow equations of the port network, as below $\forall ij \in \Omega_{\mathrm{b}}$:

$$\begin{aligned} p^{\mathrm{G}}_{i,t} - p^{\mathrm{D}}_{i,t} - p^{\mathrm{BES}_{ch}}_{\mathrm{i},t} + p^{\mathrm{BES}_{dch}}_{\mathrm{i},t} - p^{\mathrm{CHE}}_{i,t} - p^{\mathrm{Reef}}_{i,t} - p^{P2H}_{i,t} \\ = \sum_{k:j\to k} p_{jk,t} + r_{ij} l_{ij,t} - p_{ij,t} \end{aligned} \tag{20}$$

$$\begin{aligned} q^{G}_{i,t} - q^{D}_{i,t} + q^{\mathrm{Reef}}_{i,t} - q^{P2H}_{i,t} \\ = \sum_{k:j\to k} q_{jk,t} - q_{ij,t} + x_{ij} l_{ij,t} - \sum_{k:j\to k} q_{jk,t} \end{aligned} \tag{21}$$

$$u_{j,t} = u_{i,t} - 2\left(r_{ij} p_{ij,t} + x_{ij} q_{ij,t} \right) + \left(r^{2}_{ij} + x^{2}_{ij} \right) l_{ij,t}, \tag{22}$$

$$u_{i,t} = v^{2}_{i,t}, \forall i \in \Omega_{\mathrm{b}} \tag{23}$$

$$l_{ij,t} = \left(p^{2}_{ij,t} + q^{2}_{ij,t} \right) / u_{i,t} = i^{2}_{ij,t}, \tag{24}$$

$$\left\| 2p_{ij,t} \quad 2p_{ij,t} \quad l_{ij,t} - u_{i,t} \right\|_2 \le l_{ij,t} + u_{i,t} \tag{25}$$

$$v^{2}_{\min} \le u_{i,t} \le v^{2}_{\max}, \forall i \in \Omega_{\mathrm{b}} \tag{26}$$

$$i_{ij,t} \le i^{2}_{ij,\max}, \forall ij \in \Omega_{\mathrm{b}} \tag{27}$$

where constraints (20) and (21) are the active and reactive power balance equations of the port network respectively, considering the contribution and consumption of different technologies including BES, CHE, reefers, and electrolysers. These constraints along with (22)–(24) represent the relaxed branch flow equations. Eq. (25) is the relaxed model of (24). Finally, constraints (26) and (27) show the voltage and current limits. The logistics-based model of different assets in (20) and (21) are represented in the following sections.

3.2.2. Cargo handling equipment

CHEs play a vital role in port operations due to the need to move the goods from the vessels and inside the ports. Mains-connected cranes/hoppers and battery-powered IEVs are the critical elements of CHEs. In this study, a logistics-based model is proposed for the operation of CHEs, which links the operation of cranes to the IEVs.

The operation of cranes and IEVs is linked together, such that the IEVs operate if there is cargo moved from the vessels by the cranes. For

example, the operation of container tractors, reach stackers, and empty handlers follows the operation of a crane. The total consumption of a CHE located at bus i of the port network is obtained by (28), comprising of the crane power consumption, charge, and discharge power of IEVs.

$$p_{i,t}^{CHE} = \sum_{v\in\Omega_v}\sum_{c\in\Omega_c} p_{c,v,t}^{Cr} - \sum_{e\in\Omega_e}\left(p_{e,t}^{IEV_{dch}} + p_{e,t}^{IEV_{ch}}\right) \tag{28}$$

Following this equation, the logistics model of cranes is described below:

$$\sum_{c\in\Omega_c} p_{c,v,t}^{Cr} = p_{v,t}^{Ves} - p_{v,t-1}^{Ves} \tag{29}$$

$$\sum_{t\in\Omega_t} p_{v,t}^{Ves} - p_{v,tot}^{Ves} = 0 \tag{30}$$

$$0 \le p_{c,v,t}^{Cr} \le \chi_{c,v,t}^{Cr} \times p_c^{\max} \tag{31}$$

$$\chi_{c,v,t}^{Cr} = 0 \quad ,\forall t \notin [t_{ar}^{v}, t_{dep}^{v}] \tag{32}$$

where Eq. (29) represents the power consumption of crane c for unloading the vessel v. Constraints (30) demonstrate that the vessel load should be completely unloaded at the end of the operation period. Constraints (31) demonstrates the crane allocation, where binary variable $\chi_{c,v,t}^{Cr}$ indicates the crane allocation to each vessel (i.e. $\chi_{c,v,t}^{Cr} = 1$: allocated, 0:otherwise). Constraint (32) indicates that the crane allocation is only possible between the arrival and departure time of vessels.

As aforementioned, the operation of IEVs is subjected to the crane allocation. Therefore, if a crane is allocated to a vessel and unloading its goods, the IEVs start their operation. The mathematical description of the IEVs corresponding to the crane operation is described below:

$$p_{e,t}^{IEV_{dch}} = \sum_{v\in\Omega_v}\sum_{c\in\Omega_c}\left(\chi_{c,v,t}^{Cr} \times N_c^{\mathrm{IEV}}\right)\rho_e^{IEV}\, p_e^{IEV_{dch}^{\max}} \tag{33}$$

$$0 \le p_{e,t}^{IEV_{ch}} \le \left(\sum_c N_c^{IEV} - \sum_{v\in\Omega_v}\sum_{c\in\Omega_c}\left(\chi_{c,v,t}^{Cr} \times N_c^{\mathrm{IEV}}\right)\right) p_e^{IEV_{ch}^{\max}} \tag{34}$$

$$E_{e,t+1}^{IEV} = E_{e,t}^{IEV} + p_{e,t}^{IEV_{ch}}.\eta_{ch}^{IEV} - p_{e,t}^{IEV_{dch}} \big/ \eta_{dch}^{IEV} \tag{35}$$

$$0 \le \mathrm{E}_{e,t}^{\mathrm{IEV}} \le \mathrm{E}_e^{\mathrm{IEV}_{\max}} \tag{36}$$

where Eq. (33) represents the discharged power of IEV, which follows the crane allocation (i.e. $\chi_{c,v,t}^{Cr} = 1$), and it is measured by the number of IEVs allocated to each crane (i.e. N_c^{IEV}), the load factor of IEV, and maximum power consumption. The charging power of IEVs also follows the crane allocation, as indicated by (34), where the charging of an IEV happens if $\chi_{c,v,t}^{Cr} = 0$. Constraint (35) represents the energy level of IEV, which is limited by constraint (36).

3.2.3. Refeers

Refrigerated containers, which are known as reefers, are one of the main elements of port flexibility, available in large numbers in ports. Reefers can provide flexibility in forms of demand shifting and power consumption and could be considered as one of the main elements of future smart ports. The reefer operation is modelled by Eq. (37), which is measured based on the internal temperature of the reefer, and its ambient temperature. The cumulative power consumption of reefers at bus i is obtained by (38). Constraint (39) represents the temperature limits of reefer r. Finally, constraint (40) limits the power consumption of the reefer.

$$T_{r,t+1}^{Reef} = T_{r,t}^{Reef} - \beta_r p_{r,t}^{\mathrm{Reef}} + \alpha_r\left(T_{r,t}^{\mathrm{amb}} - T_{r,t}^{Reef}\right) \tag{37}$$

$$p_{i,t}^{\mathrm{Reef}} = \sum_{r\in\Omega_r} p_{r,t}^{\mathrm{Reef}} \tag{38}$$

$$T_{r,\min}^{Reef} \le T_{r,t}^{Reef} \le T_{r,\max}^{Reef} \tag{39}$$

$$0 \le p_{r,t}^{\mathrm{Reef}} \le p_{r,\max}^{\mathrm{Reef}} \tag{40}$$

3.2.4. Battery energy storage

Battery energy storage can provide a great share of flexibility to the ports. Their charge and discharge power can be controlled based on available power and price signals. This paper considers the following model for the operation of the BES [33].

$$\mathrm{SOC}_{i,t+1}^{\mathrm{BES}} = \mathrm{SOC}_{i,t}^{\mathrm{BES}} + p_{i,t}^{BES_{ch}} \cdot \eta_{ch}^{BES} - p_{i,t}^{BES_{dch}} \big/ \eta_{ch}^{BES} \tag{41}$$

$$0 \le \mathrm{SOC}_{i,t}^{\mathrm{BES}} \le \mathrm{SOC}_{i,\max}^{\mathrm{BES}} \tag{42}$$

$$0 \le p_{i,t}^{\mathrm{BES}_{ch}} \le \chi_{i,t}^{BES_{ch}} \times P_{\mathrm{i,max}}^{\mathrm{BES}_{ch}} \tag{43}$$

$$0 \le p_{i,t}^{\mathrm{BES}_{dch}} \le \chi_{i,t}^{BES_{dch}} \times P_{\mathrm{i,max}}^{\mathrm{BES}_{dch}} \tag{44}$$

$$\chi_{i,t}^{BES_{ch}} + \chi_{i,t}^{BES_{dch}} \le 1 \tag{45}$$

where constraint (41) represents the state of charge of BES; constraint (42) shows the maximum state of charge of BES; constraints (43) and (44) are the charge and discharge power limits of BES respectively, where binary variables $\chi_{i,t}^{BES_{ch}}$ and $\chi_{i,t}^{BES_{dch}}$ indicate the charge–discharge status; constraint (45) prevents the simultaneous charge and discharge.

3.2.5. Green hydrogen production and storage

Producing hydrogen from renewable energy (known as green hydrogen) offers ports a plethora of environmental and economic advantages. Smart seaports can play a pivotal role in the hydrogen market by serving as a crucial connector between the origins and destinations of hydrogen. This strategic positioning can enable them to exploit their potential in producing hydrogen, thanks to their proximity to offshore wind farms. Ports can host different production and storage facilities for hydrogen, functioning as central hubs for fuel bunkering. The incorporation of P2H technologies into smart ports is feasible through the installation of electrolyser, which is the main core of P2H, and extracts hydrogen from water using the electric energy [34].

Based on this idea, this paper aims to leverage the potential of ports in increasing the utilisation of wind power generation by producing hydrogen from excess wind power. Envisaging a future scenario, where the hydrogen-powered vessels play a vital role in the transaction of goods, the demand for hydrogen is defined based on the number of vessels in the port. Expanding upon this concept, Eq. (46) [35] defines the demand for hydrogen, factoring in the engine size of each vessel and the number of vessels at berth, as represented below:

$$H_{i,t}^{D} = \Delta t \frac{\sum_{v\in\Omega_v}\left(N_t^V \times P_v^{en} \times t_v^{op}\right) \times 3600}{\eta \times LHV} \tag{46}$$

where P_v^{en} defines the engine power in kW of vessel v; N_t^V is the number of vessels at berth at time period t; t_v^{op} is the operating time of vessel v in hours; η is the efficiency; LHV represents the lower heating value of hydrogen to determine the hydrogen consumption, which is 120,000 kJ/kg. Knowing the engine power of the vessels, their operating time for a certain voyage, and their arrival and departure data enables the calculation of total hydrogen demand based on (46).

Assuming the availability of off-shore wind farms, the extra wind power generation in the main grid can be used as the source for producing hydrogen. Utilising the proton exchange membrane electrolyser, which has several advantages such as high efficiency and pollution-free operation [36], the produced hydrogen can be obtained as follows [28]:

$$H_{i,t}^{G} = \xi_i^{P2H} \times \left(p_{i,t}^{P2H} + p_{i,t}^{WT_c}\right) \tag{47}$$

where (47) shows the extractable hydrogen (in kg). The electrolyser efficiency (i.e. ξ_i^{P2H}) is a function of the loading level, as shown below [28]:

$$\xi_i^{P2H} = f\left(p_i^{P2H}\right) = \xi_{i,\max}^{P2H} - \frac{\xi_{i,\max}^{P2H} - \xi_{i,\min}^{P2H}}{p_{i,\max}^{P2H} - p_{i,\min}^{P2H}}\left(p_i^{P2H} - p_{i,\min}^{P2H}\right) \tag{48}$$

$$p_{i,\min}^{P2H} \le p_i^{P2H} \le p_{i,\max}^{P2H} \tag{49}$$

Finally, based on the production and demand equations in (46) and (47), and capacity of hydrogen storage, the following nodal hydrogen balance can be expressed for each port.

$$H_{i,t}^{S} = H_{i,t-1}^{S} + \Delta t \left(\eta_c^H H_{i,t}^{G} - \frac{1}{\eta_d^H} H_{i,t}^{D} \right) \tag{50}$$

$$H_i^{Min} \le H_{i,t}^{S} \le H_i^{\max} \tag{51}$$

where (50) denotes the nodal hydrogen balance. $H_{i,t}^{S}$, $H_{i,t}^{G}$, and $H_{i,t}^{D}$ are the storage capacity of the tank connected to the electrolyser, generated hydrogen by electrolyser and demand for hydrogen based on (46), respectively. Constraint (51) limits the storage capacity of the tank connected to the electrolyser.

4. Multi-port coordination optimisation

After realising the network operation parameters, the MGO performs the following optimisation to define the flexibility requirements from the ports:

$$\min_{DV} OF^{MGO} = \min \left\{ \begin{pmatrix} C_{ThG}^{Op} + C_{WT}^{Op} + C_{WT}^{Cur} + C_{GP}^{\mathrm{Res}} \\ + C_{ThG}^{Em} \end{pmatrix} \right\} \tag{52}$$

Subject to :

$$E^{MGO}(X_{DV}^{MGO}) \le 0 \tag{53}$$

$$G^{MGO}(X_{DV}^{MGO}) = 0 \tag{54}$$

where (52) is the objective function of the MGO (represented in (1)), and constraints (53) and (54) represent the equality and inequality constraints of the MGO optimisation, which are presented in constraints (2)–(16). The decision variables of MGO optimisation are represented by X_{DV}^{MGO}. After solving the optimisation model, the optimal values of $\vartheta_{b,t}^{Flex}$ and $P_{b,t}^{WT_c}$ are reported to the port operators.

Based on the information provided by the MGO and logistics-operation parameters of the port network, the operators run the following optimisation:

$$\min\nolimits_{DV} OF^{port} = \sum_{t \in \Omega_t} \Delta t \times \left(C_t^{port} - R_t^{port} \right) \tag{55}$$

subject to :

$$E^{PO}(X_{DV}^{PO}) \le 0 \tag{56}$$

$$G^{PO}(X_{DV}^{PO}) = 0 \tag{57}$$

where (55) is the objective function of the port optimisation (i.e. (17)–(19)), while (56) and (57) denotes the equality and inequality constraints of the port network, represented by (20)–(49). After solving this optimisation, the port operator sends the value and price of flexibility along with the amount of wind power that can be used for producing hydrogen.

4.1. Multi-port flexibility coordination

The determination of the value of flexibility offered by individual ports is carried out through a coordination system that receives information from ports based on their logistics operation. In this system, each port acts as a participant and submits its supply curves to an independent coordinator. On the other side, MGO provides a single-step demand curve for each hour to the market, representing the required demand with a price cap set by a maximum value determined in the previous section. The flexibility coordinator is responsible for deriving the value of flexibility, which is optimally obtained by solving an optimisation problem based on merit orders, as formulated in the Algorithm 1.

The algorithm operates iteratively, addressing the unique characteristics of each hour of a day. It incorporates inputs from all ports, considering their respective supply curves, optimal offers (G_t^p), corresponding prices (λ_t^O), and the flexibility demand from the MGO, along with the associated price cap ($\overline{\lambda_t}$). The primary objective is to minimise the cost of satisfying the port's demand by effectively matching it with the available flexibility. This optimisation is subject to the condition that accepted offers fall within the range of maximum offers provided by each port, and the flexibility demand is met. The auxiliary variable y_t serves as a representation of the unfulfilled flexibility required by the MGO, and the norm operator $|\cdot|_1$ is employed for vector calculations.

Upon solving the optimisation problem for each hour, the coordinator communicates the determined price and commitments made by each port. Additionally, the operator receives information concerning the overall flexibility that can be provided by each port, along with the corresponding flexibility price. In cases where the acquired values do not align with the MGO's requirements, necessary adjustments are undertaken, prompting the initiation of a new iteration.

The algorithm, encapsulated in Algorithm 1, takes the flexibility demand D_t as input for each hour $t = 1$ to 24 and outputs optimal offers O_t for the corresponding hours. The optimisation problem within the algorithm seeks to minimise the expression $G_t^p \cdot \lambda_t^O + \bar{\lambda}_t \cdot y_t$ subject to certain constraints, ensuring that the accepted offers align with port limitations and fulfil the flexibility demand.

Algorithm 1: Multi-port Flexibility Coordination

Input: Flexibility demand D_t for each hour $t = 1$ to 24
Output: Optimal offers O_t for each hour $t = 1$ to 24
for $t = 1$ *to* 24 **do**
  Solve the following optimisation problem:

  $\min \left(G_t^p \cdot \lambda_t^O + \bar{\lambda}_t \cdot y_t \right)$

  subject to:

  $0 \le G_t^p \le O_t$

  $D_t = \|G_t^p\|_1 + y_t : \pi_t$

  Output: G_t^p as the vector of accepted offers and π_t as clearing price for hour t
end

5. Simulation setup and test system

The framework of the proposed optimisation model is given in Fig. 2. As can be seen in this figure, the MGO and port operators solve their optimisation with the aim of minimising the total cost of operating the system including the emission cost. The MGO optimisation in this level determines the optimal power flow decision variables, as well as the value of wind curtailment and the flexibility requirement from the ports. Simultaneously, the port optimisation problems define the optimal coordination of logistics-electric operation along with a supply curve indicating the price and value of the flexibility that can be provided by each port. The MPFC receives the requirements of the MGO, and based on the information provided by the ports including the supply curves, defines the value of flexibility and the amount of wind power curtailment which can be used in the ports. These processes are numbered with one in Fig. 2. The MPFC receives this information and solves an optimisation based on Algorithm 1. The share of each port in providing the required flexibility and the hourly price of flexibility is reported to the MGO and port operators at this level. Based on this information, the port operators provide the required flexibility for the

Table 1
Hourly power demand and wind power generation [37].

Time	Active power demand (MW)	Reactive power demand (MVAr)	Wind generation (MW)
t_1	5022	1114	253
t_2	4678	1038	263
t_3	4472	992	295
t_4	4018	891	299
t_5	3770	836	331
t_6	4087	906	348
t_7	4541	1007	367
t_8	5091	1129	349
t_9	5160	1144	406
t_{10}	5917	1312	455
t_{11}	6260	1388	468
t_{12}	6604	1465	498
t_{13}	6329	1404	490
t_{14}	5710	1266	473
t_{15}	5504	1221	441
t_{16}	5641	1251	404
t_{17}	5848	1297	372
t_{18}	6192	1373	402
t_{19}	6467	1434	409
t_{20}	6549	1453	417
t_{21}	6673	1480	446
t_{22}	6880	1526	500
t_{23}	6260	1388	461
t_{24}	5710	1266	418

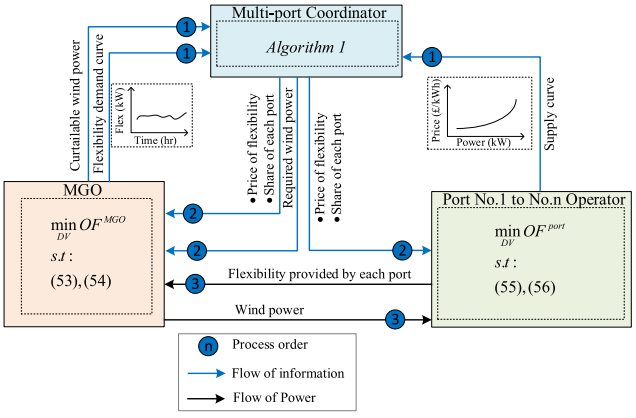

Fig. 2. The process of solving the proposed multi-port coordination problem.

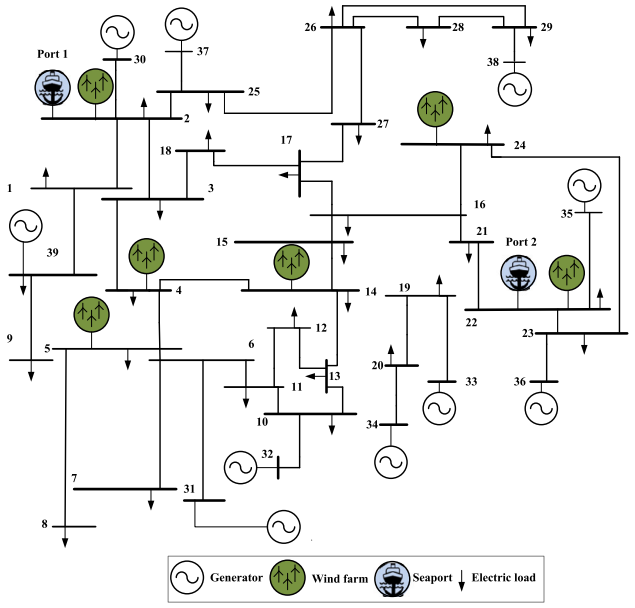

Fig. 3. One-line diagram of the main grid consisting of the buses connecting the seaports.

main grid while receiving the wind power to supply their electrolyser. It is worth mentioning that since this paper mainly focuses on port flexibility, the participation of other flexibility providers has not been considered.

The proposed model is a mixed integer linear programming that has been solved using the CPLEX solver in GAMS software. The IEEE 39-bus network is chosen as the main grid in this paper. Fig. 3 illustrates the one-line diagram of this network. Six wind farms each with a maximum capacity of 500 MW are installed at buses 2, 4, 5, 14, 22, and 24. Active and reactive demand as well as available wind power capacity at each hour is given in Table 1 [37].

Two seaports are assumed to be at buses 2 and 22 of the network, where the availability of wind farms provides a potential green hydrogen production for ports. In the rest of this paper, the ports connected to buses 2 and 22 are called Port 1 and 2 respectively. The one-line diagram of the Port 1 network is given in Fig. 4. This network is connected to Bus 2 of the main grid. The data of different assets, including different berths, cranes, IEVs, ES, and RESs is taken from [31]. For additional details regarding the operation of the port, refer to [31]. Without loss of generality, to investigate the proposed multi-port coordination optimisation problem, a second port is defined based on Port 1 data, accounting for variations in asset sizes and vessel arrival times. This port is called Port 2 and it is connected to Bus 22 of the main grid. The parameters related to the port assets are given in Table 2 [31]. The data of P2H units installed at each port is given in Table 3 [28].

6. Results and discussion

In this section, the effectiveness of the presented methodology is thoroughly examined. The goal is to validate and demonstrate the importance of the proposed method by comparing its performance in different case studies. Specifically, the focus lies on exploring the crucial aspects of multi-port coordination, hydrogen production, and the environmental benefits associated with the cooperation of the ports. The presented approach can be investigated from various perspectives, such as economic and environmental benefits, how the flexibility of

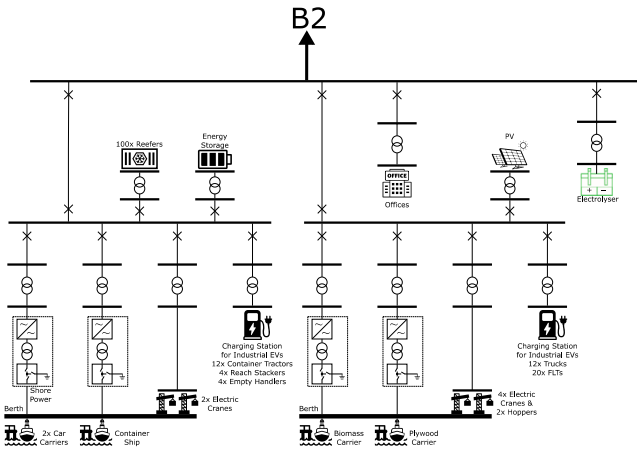

Fig. 4. Port 1 electricity network including different assets.

Table 2
Technical parameters PoT assets [31].

Parameter	Value (unit)	Parameter	Value (unit)
$p_e^{\max}$	82.2 (kW)	$p_{r,\max}^{\text{Reef}}$	5.7 (kW)
$T_{r,\max}^{Reef}$	−28 (°C)	$T_{r,\min}^{Reef}$	−30 (°C)
α_r	2.903	β_r	0.054 (°C/kW)
ρ_e^{IEV}	0.5	$p_i^{pv_{max}}$	752 kW
$P_{i,max}^{BES_{ch/dch}}$	500 (kW)	$SOC_{i,max}^{BES}$	1000 (kW)
$p_e^{IEV_{ch/dch}^{\max}}$	100 (kW)	$E_e^{IEV_{max}}$	200 (kW)
$\eta_{ch/dch}^{BES}$	95 (%)	wf	50 ($/person)

the ports impacts their operation and coordination, and the role of the presented framework in leveraging the potential of ports for green hydrogen production. This section demonstrates and explores these perspectives by considering three cases, as outlined below:

Case I: The proposed port multi-port coordination method serves as the main case study, providing a benchmark for comparison.

Case II: The proposed method without the coordination framework. This case study will be compared with Case I to show the importance of the proposed multi-port coordination method.

Additionally, a sensitivity analysis is conducted to further examine the impact of critical inputs on the demonstrated results of the model. Through these comprehensive analyses and comparisons, this section sheds light on the effectiveness of the presented methodology in facilitating coordination, environmental and economic benefits of port cooperation, and harnessing the potential of ports for green hydrogen.

6.1. Environmental and economic perspectives

To facilitate port cooperation, the MPFC is introduced, where the required flexibility from MGO, along with a price cap, is specified. The specific values for the required flexibility (referred to as process one in Fig. 2) for the chosen case study are provided in Fig. 5. It is imperative to note that if spinning reserve from thermal generation units is utilised, it would result in approximately 7500 kgCO_2/day. With the system's long-term operation in view, this number could potentially increase further. Hence, the assumption is that MGO prioritises the flexibility provided by ports, but with a price cap in place to prevent a significant increase in the cost of electricity provision.

Each port independently undergoes their optimisation problem to determine their hourly supply curve. This is illustrated in Fig. 6 for selected hours, showcasing the supply curves generated by both ports. Upon observing the figure, it becomes evident that while Port 2 has

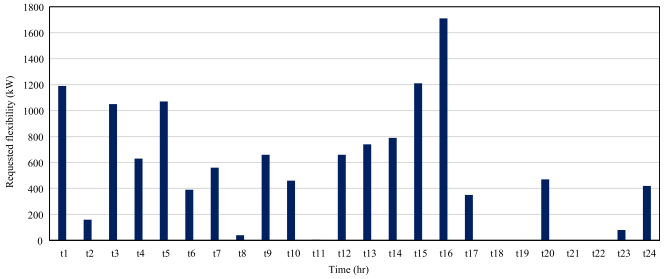

Fig. 5. The flexibility requested by the MGO from the ports.

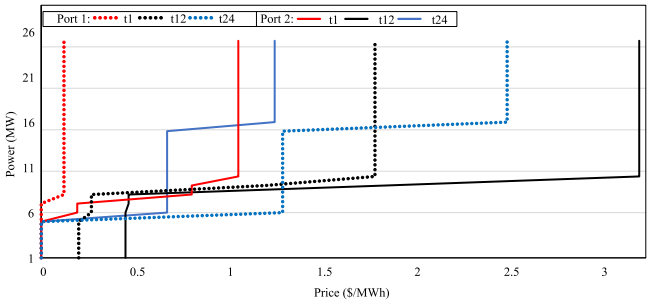

Fig. 6. The supply curves offered by the ports for three different hours.

the potential to offer greater flexibility, the price for that flexibility is higher compared to Port 1 for most hours. However, during periods when a larger degree of flexibility is required, the market clearing price is influenced by the supply curves of Port 2. Fig. 6 vividly portrays diverse supply curves from both ports across various hours. It is essential to highlight the varying assets each port possesses during different times, granting flexibility in adjusting consumption for that specific hour. The cost or price associated with these performance variations is derived from Section 4 formulation (Eqs. (52)–(57)), allowing each port to determine the price corresponding to different levels of flexibility. Examining Fig. 6, it can be observed that during certain periods (e.g., $t1$), ports exhibit lower flexibility due to the limited asset availability. Both ports can supply a reduced amount of power, resulting in higher prices. Conversely, at time period $t12$, flexibility is heightened, enabling ports to provide more power at lower prices. These supply curves are subsequently utilised to meet grid demand, determining the overall price of port flexibility cleared through the coordination of MGO and ports.

To address this, the MPFC is responsible for solving Algorithm 1 for each hour. The output of this algorithm provides each port with its respective share in providing the required flexibility, as depicted in Fig. 7. This figure demonstrates that the requested flexibility from the MGO is met by the ports, except for the time denoted as t_1, which is primarily due to insufficient available generation and flexible load. Thus, it can be concluded that future electrified ports can actively participate in the energy network, presenting a viable alternative to current passive ports. This approach can delay the need for additional generation and transmission investments while meeting environmental pollution standards.

Fig. 8 displays the flexibility price determined by the MPFC for each hour. These prices are derived from the supply curves submitted by port operators (refer to Fig. 6). As indicated in the figure, the prices set by the MPFC are all below the price cap. On average, the daily price established by the MPFC is approximately 50% lower than the price cap. This implies that the proposed MPFC serves as an effective method for defining port flexibility cooperation.

In order to show the economic benefits of the proposed method in addition to its environmental advantages (i.e. reducing 7500

Table 3
Data of P2H units [28].

Port No.	$p^{P2H}_{i,\min}$ (MW)	$p^{P2H}_{i,\max}$ (MW)	$\gamma_{0,i}$ ($/h)	$\gamma_{1,i}$ ($/MWh)	$\kappa_{0,i}$ ($/h)	$\kappa_{1,i}$ ($/kg)	$\xi^{P2H}_{i,\min}$ (kg/MWh)	$\xi^{P2H}_{i,\max}$ (kg/MWh)
Port 1	0	700	9800	1.20	0	3	20	15
Port 2	0	1400	19,600	1.20	0	3	20	15

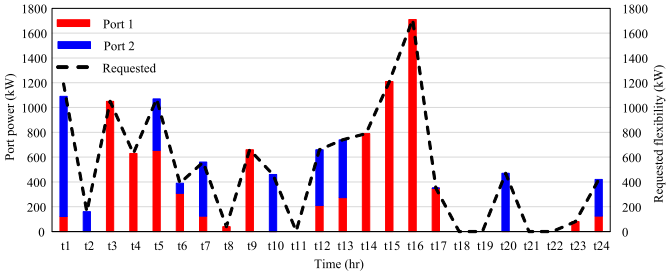

Fig. 7. Share of each port for providing flexibility requested by the main grid.

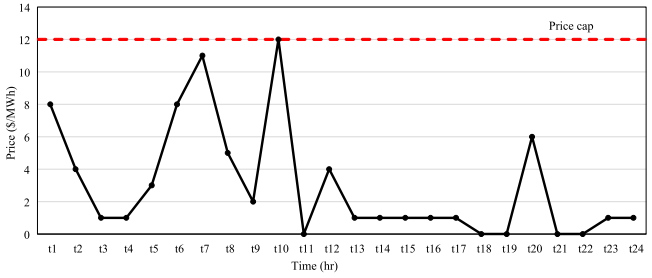

Fig. 8. Price of flexibility defined by the MPFC.

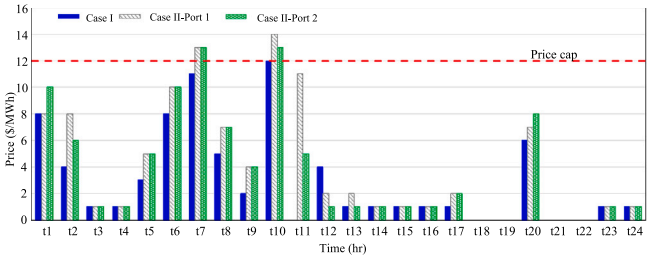

Fig. 9. Price of flexibility in cases I and II.

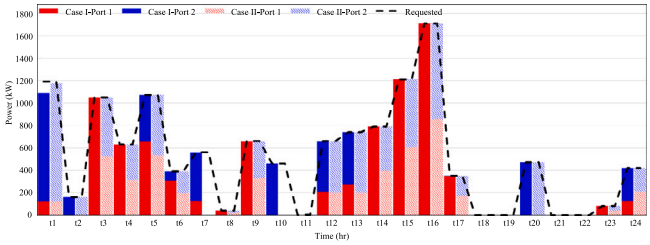

Fig. 10. Share of each port in providing the requested power by the MGO in cases I and II.

$kgCO_2$/day as demonstrated in Fig. 5), the difference between price cap and the price defined by the MPFC in Fig. 8 is multiplied by the flexibility required by the MGO, i.e.: $\{\sum_t (|\bar{\lambda}_t - G^p_t|) \times P^{Res}_t\}$; which is equal to \$109.9 per day. Considering the cost of wind power curtailment prevented by supplying the ports, the MGO can decrease their operational cost by \$39,225.9, while port operators make \$3707.8 income from the provision of flexibility and providing hydrogen to the vessels. These figures clearly show the significance of coordinating the port flexibility from environmental and economic perspectives for both port and main grid operators.

6.2. Role of multi-port flexibility coordinator

The proposed MPFC framework plays a crucial role in optimising the environmental and economic objectives of ports while complying with the requirements of the MGO. This section compares cases I and II to investigate the necessity of the MPFC method. In Case II, the MPFC algorithm is not solved and the MGO directly sends its required flexibility along with the price cap to the ports. The ports send their supply curves and the MGO decides how much they want to buy from each operator. For example, at time t_1, the MGO requested 1.19 MW flexibility from the ports (see Fig. 5); and ports 1 and 2 respectively can provide this flexibility with 10 and 8 \$/MWh based on supply curves in Fig. 6. This means the MGO buys different amounts of flexibility from the ports with different prices in the lack of an optimised MPFC.

The hourly price of flexibility in cases I and II (i.e. with and without MPFC) is shown in Fig. 9. As can be seen in this figure, the price of flexibility in Case II is different from that of Case I, while the price defined in the former is higher than that of the latter in most of the studied intervals. More dramatically, at time slots t_7 and t_{10} the price determined in Case II is above the price cap. This means the MGO has to use thermal generation units to provide such flexibility in those times, which gives rise to environmental pollution. To demonstrate the effectiveness of the proposed method in Case I, the share of each port in providing the requested flexibility is depicted in Fig. 10. This figure illustrates the lack of competition between the ports in Case II, with no power exchange between the ports and the main grid at the intervals t_7 and t_{10}. This leads to a decrease in environmental impact to $kgCO_2$/day, demonstrating the efficacy of the proposed method in Case I by creating competition between the ports and mitigating environmental emissions.

Table 4 summarises the economic and environmental figures of cases I and II. As can be seen in this figure, the proposed method in Case I suggested better economic and environmental results compared to that of Case II. It is worth mentioning that considering a long-term operation and involvement of a large number of ports in such a coordination method can highlight its advantages to a greater extent.

6.3. Harnessing Green hydrogen

Previous sections highlighted the importance of the proposed coordination framework and the economic and environmental advantages of port flexibility. This section investigates the potential of ports in harnessing green hydrogen and their role in increasing the penetration level of RESs.

Fig. 11 shows the curtailed power used by the P2H units in the ports. As can be seen in this figure, all curtailable power reported by the MGO is used in the P2H units. This figure shows the significance of hydrogen production in the ports in increasing the penetration level of RESs. Based on Fig. 11 and objective functions of the MGO and port operators (i.e. Eqs. (1), and (17)), the MGO decreased its operational cost by \$39,116 while port operators make \$3667 from using the curtailable wind power. The former is because the MGO does not have to pay for wind power curtailment costs while the latter is due to the income port operators can make from turning the power to hydrogen. The produced power by electrolyser is saved in the hydrogen storage and supplies the

Table 4
Comparison of cases I and II.

Case No.	Cost saving ($/day)	Daily average difference with the price cap (%)	CO_2 saving $kgCO_2$/day
Case I	109.9	50	7500
Case II	102.5	48	6888

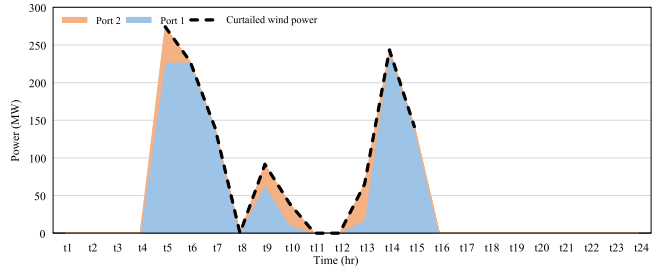

Fig. 11. The curtailed wind power used by the P2H units.

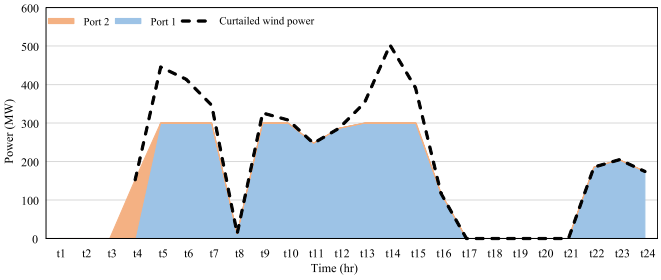

Fig. 12. The curtailed wind power used by the P2H units with consideration for branch capacity limit.

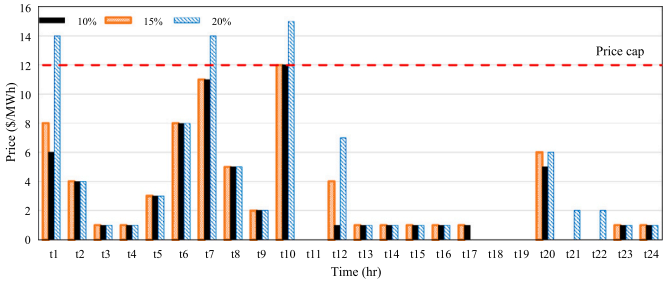

Fig. 13. Variation of flexibility price for different values of flexibility requested from the MGO.

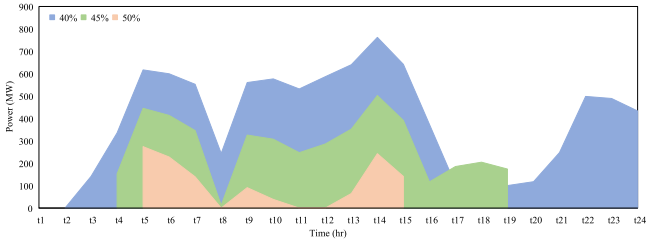

Fig. 14. The changes in utilisation of curtailable wind power by ports for different levels of wind power penetration.

vessels at berth. It is worth mentioning that the rest of the power for producing the hydrogen is provided locally in the ports.

Fig. 11, however, illustrates the results for the IEEE 39-bus network with high branch capacity limits. To showcase the impact of line congestion on P2H, Fig. 12 is presented, taking into account a maximum capacity of 3 MW in the branches linking the electrolysers in the ports to the main grid. This figure demonstrates that power transfer limits can influence the transmission of power from the main grid to the electrolysers. It can be seen that ports failed to convert all available curtailed wind power to the hydrogen due to the branch capacity limit. It emphasises the importance of incorporating branch capacity considerations in investment planning schemes for ports, enabling their participation in flexibility programs.

6.4. Sensitivity analysis

This section provides different sensitivity analyses on the critical information in the proposed method. Fig. 13 shows the changes in the flexibility price defined by the MPFC when the percentage of flexibility requested from the MGO changes from 10% to 20%. As can be seen in this figure, when the value of flexibility requested by the MGO increases to 20%, the port prices exceed the price cap, meaning that the port capacity is not enough for the requested flexibility value and they cannot provide it with the suggested MGO price cap. Therefore, the amount of flexibility that can be provided by ports is limited by their size.

Finally, Fig. 14 shows the changes in storage of curtailable wind power by P2H units in the ports for different levels of wind power penetration set by the MGO. Based on this figure, if for any security reason, the MGO decides to decrease the penetration level of wind in the network, the P2H units in the ports can store and use all available wind power. Furthermore, this figure demonstrates that decreasing the penetration level by 5% (i.e. from 45% to 40%) can bring about more benefit for the ports in terms of P2H, with about 52% increase in the amount of hydrogen production/storage from potential wind power reported as curtailable by the MGO.

7. Conclusion

This paper proposes a comprehensive coordination framework for the seamless integration of port flexibility into the energy network through the concept of green port-to-grid. The proposed method meticulously considers the logistics-electric constraints of the ports while ensuring a harmonious balance with the operational and physical limits of the main grid. A multi-port flexibility coordination framework is proposed for defining the price and value of flexibility each port can provide for the main grid. Furthermore, the potential of producing and storing hydrogen in ports is investigated taking into account the availability of vessels at berth as the consumers of green hydrogen. The effectiveness of the proposed method is studied from economic and environmental perspectives to highlight its advantages. The simulation results show a reduction of 7500 $kgCO_2$/day as a result of utilising the port coordination framework, which is an important guideline for future smart ports to follow. The port flexibility prices defined by the multi-port flexibility coordination operator are 50% less than the price cap sent by the main grid operator. This enables the active participation of the ports in the flexibility while highlighting the significance of port cooperation. Finally, the ports enabled the utilisation of 100% curtailable wind power through producing and storing hydrogen, which can bring about more income for the ports and decrease the cost of wind power curtailment for the main grid operator.

The future research direction can focus on the long-term technical and economic advantages of the proposed coordination framework.

This will involve a more extensive simulation analysis to explore the enduring impact of port flexibility coordination, addressing aspects such as generation and transmission planning while highlighting its sustained environmental benefits. Exploring the optimal number of participating ports in the collaborative algorithm could be a promising direction for future research, enhancing the efficiency of flexibility provision within the grid. Finally, Future research could investigate deeper into the collaborative interactions among different ports within the multi-port coordination framework. This includes exploring potential strategic games between ports and investigating specific exchanges of physical quantities among them for a more comprehensive understanding of the collaborative control dynamics.

CRediT authorship contribution statement

Saman Nikkhah: Conceptualization, Data curation, Formal analysis, Methodology, Resources, Software, Validation, Visualization, Writing – original draft, Writing – review & editing. **Arman Alahyari:** Conceptualization, Data curation, Formal analysis, Funding acquisition, Methodology, Resources, Software, Validation, Visualization, Writing – original draft, Writing – review & editing. **Abbas Rabiee:** Conceptualization, Data curation, Formal analysis, Software, Supervision, Validation, Writing – review & editing. **Adib Allahham:** Conceptualization, Formal analysis, Funding acquisition, Resources, Writing – review & editing. **Damian Giaouris:** Funding acquisition, Project administration, Resources, Supervision, Writing – review & editing.

Declaration of competing interest

The authors declare that they have no known competing financial interests or personal relationships that could have appeared to influence the work reported in this paper.

Data availability

Data will be made available on request.

Acknowledgment

This work was supported by the Newcastle University and Engineering and Physical Sciences Research Council under Grant EP/S00078X/2: Supergen Energy Networks Hub Accleration Flex Fund.

References

[1] Port freight annual statistics. Department for Transport; 2021, https://www.gov.uk/government/statistics/port-freight-annual-statistics-2021, addendum ="2022".
[2] Fourth IMO gHG study. International Maritime Organisation; 2020, https://www.imo.org/en/OurWork/Environment/Pages/Fourth-IMO-Greenhouse-Gas-Study-2020.aspx.
[3] Final uk greenhouse gas emissions national statistics: 1990 To 2019. Department for Business Energy and Industrial Strategy, [Online]. Available: https://www.gov.uk/government/statistics/final-uk-greenhouse-gas-emissions-national-statistics-1990-to-2019.
[4] Clean maritime plan: Maritime 2050 environment route map. Department for Transport and Maritime and Coastguard Agency, [Online]. Available: https://www.gov.uk/government/publications/clean-maritime-plan-maritime-2050-environment-route-map.
[5] Brooks M, McCalla R, Pallis A, Van De Lugt L. Cooperation and coordination in strategic port management: the case of atlantic canada's ports. Can J Transp 2010;4(1):29–42.
[6] Ma Q, Jia P, She X, Haralambides H, Kuang H. Port integration and regional economic development: Lessons from china. Transp Policy 2021;110:430–9.
[7] Theo Notteboom J-PR. Athanasios pallis. In: Port economics, management and policy. 2022.
[8] Fang S, Xu Y, Li Z, Zhao T, Wang H. Two-step multi-objective management of hybrid energy storage system in all-electric ship microgrids. IEEE Trans Veh Technol 2019;68(4):3361–73.
[9] Kanellos FD, Tsekouras GJ, Hatziargyriou ND. Optimal demand-side management and power generation scheduling in an all-electric ship. IEEE Trans Sustain Energy 2014;5(4):1166–75.
[10] Golias MM, Saharidis GK, Boile M, Theofanis S, Ierapetritou MG. The berth allocation problem: Optimizing vessel arrival time. Marit Econ Logist 2009;11:358–77.
[11] Iris Ç, Lam JSL. Optimal energy management and operations planning in seaports with smart grid while harnessing renewable energy under uncertainty. Omega 2021;103:102445.
[12] Yu J, Voß S, Song X. Multi-objective optimization of daily use of shore side electricity integrated with quayside operation. J Clean Prod 2022;351:131406.
[13] Peng Y, Dong M, Li X, Liu H, Wang W. Cooperative optimization of shore power allocation and berth allocation: A balance between cost and environmental benefit. J Clean Prod 2021;279:123816.
[14] Hein K, Xu Y, Gary W, Gupta AK. Robustly coordinated operational scheduling of a grid-connected seaport microgrid under uncertainties. IET Gener Transm Distrib 2021;15(2):347–58.
[15] Wang X, Huang W, Wei W, Tai N, Li R, Huang Y. Day-ahead optimal economic dispatching of integrated port energy systems considering hydrogen. IEEE Trans Ind Appl 2021;58(2):2619–29.
[16] Molavi A, Shi J, Wu Y, Lim GJ. Enabling smart ports through the integration of microgrids: A two-stage stochastic programming approach. Appl Energy 2020;258:114022.
[17] Chen Z, Fan F, Tai N, Li C, Zhang X. Multi-objective voltage/var control for integrated port energy system considering multi-network integration. Int J Electr Power Energy Syst 2023;150:109092.
[18] Gennitsaris SG, Kanellos FD. Emission-aware and cost-effective distributed demand response system for extensively electrified large ports. IEEE Trans Power Syst 2019;34(6):4341–51.
[19] Yadegari S, Abdi H, Nikkhah S. Risk-averse multi-objective optimal combined heat and power planning considering voltage security constraints. Energy 2020;212:118754.
[20] Mao A, Yu T, Ding Z, Fang S, Guo J, Sheng Q. Optimal scheduling for seaport integrated energy system considering flexible berth allocation. Appl Energy 2022;308:118386.
[21] Kanellos FD, Volanis E-SM, Hatziargyriou ND. Power management method for large ports with multi-agent systems. IEEE Trans Smart Grid 2017;10(2):1259–68.
[22] Li M, Du W, Nian F. An adaptive particle swarm optimization algorithm based on directed weighted complex network. Math Probl Eng 2014;2014.
[23] Tao Y, Qiu J, Lai S, Sun X, Zhao J. Flexible voyage scheduling and coordinated energy management strategy of all-electric ships and seaport microgrid. IEEE Trans Intell Transp Syst 2022.
[24] Sun X, Qiu J, Tao Y, Yi Y, Zhao J. Distributed optimal voltage control and berth allocation of all-electric ships in seaport microgrids. IEEE Trans Smart Grid 2022;13(4):2664–74.
[25] Peng Y, Li X, Wang W, Liu K, Bing X, Song X. A method for determining the required power capacity of an on-shore power system considering uncertainties of arriving ships. Sustainability 2018;10(12):4524.
[26] Kumar J, Mekkanen M, Karimi M, Kauhaniemi K. Hardware-in-the-loop testing of a battery energy storage controller for harbour area smart grid: A case study for vaasa harbour grid. Energy Rep 2023;9:447–54.
[27] Akhlaghi M, Moravej Z, Bagheri A. Maximizing wind energy utilization in smart power systems using a flexible network-constrained unit commitment through dynamic lines and transformers rating. Energy 2022;261:124918.
[28] Rabiee A, Keane A, Soroudi A. Green hydrogen: A new flexibility source for security constrained scheduling of power systems with renewable energies. Int J Hydrog Energy 2021;46(37):19270–84.
[29] Requirement to turn off wind turbines is costing brits hundreds of millions. Sky News, [Online]. Available: https://tvpworld.com/67525278/requirement-to-turn-off-wind-turbines-is-costing-brits-hundreds-of-millions.
[30] Vahidinasab V, Nikkhah S, Allahham A, Giaouris D. Boosting integration capacity of electric vehicles: a robust security constrained decision making. Int J Electr Power Energy Syst 2021;133:107229.
[31] Sarantakos I, Bowkett A, Allahham A, Sayfutdinov T, Murphy A, Pazouki K, Mangan J, Liu G, Chang E, Bougioukou E, Patsios H. Digitalization for port decarbonization: Decarbonization of key energy processes at the port of tyne. IEEE Electrif Mag 2023;11(1):61–72.
[32] Farivar M, Low SH. Branch flow model: Relaxations and convexification—part i. IEEE Trans Power Syst 2013;28(3):2554–64.
[33] Nasr M-A, Nikkhah S, Gharehpetian GB, Nasr-Azadani E, Hosseinian SH. A multi-objective voltage stability constrained energy management system for isolated microgrids. Int J Electr Power Energy Syst 2020;117:105646.
[34] Allahham A, Greenwood D, Patsios C, Walker SL, Taylor P. Primary frequency response from hydrogen-based bidirectional vector coupling storage: Modelling and demonstration using power-hardware-in-the-loop simulation. Front Energy Res 2023;11:1217070.
[35] How much hyrdogen do i need for the fuel cell on my ship. Marine Serivice Noord, [Online]. Available: https://marine-service-noord.com/en/products/alternative-fuels-and-technologies/hydrogen/how-much-hydrogen-do-i-need/.
[36] Gößling S, Stypka S, Bahr M, Oberschachtsiek B, Heinzel A. Proton exchange membrane water electrolysis modeling for system simulation and degradation analysis. Chem Ing Tech 2018;90(10):1437–42.
[37] Rabiee A, Keane A, Soroudi A. Technical barriers for harnessing the green hydrogen: A power system perspective. Renew Energy 2021;163:1580–7.